

Chapter 14

A Model of Evolutionary Dynamics with Quasiperiodic Forcing

Elizabeth Wesson and Richard Rand

Abstract Evolutionary dynamics combines game theory and nonlinear dynamics to model competition in biological and social situations. The replicator equation is a standard paradigm in evolutionary dynamics. The growth rate of each strategy is its excess fitness: the deviation of its fitness from the average. The game-theoretic aspect of the model lies in the choice of fitness function, which is determined by a payoff matrix.

Previous work by Ruelas and Rand investigated the Rock-Paper-Scissors replicator dynamics problem with periodic forcing of the payoff coefficients. This work extends the previous to consider the case of quasiperiodic forcing. This model may find applications in biological or social systems where competition is affected by cyclical processes on different scales, such as days/years or weeks/years.

We study the quasiperiodically forced Rock-Paper-Scissors problem using numerical simulation, and Floquet theory and harmonic balance. We investigate the linear stability of the interior equilibrium point; we find that the region of stability in frequency space has fractal boundary.

Keywords Replicator equation • Quasiperiodic forcing • Floquet theory • Harmonic balance • Numerical integration

14.1 Introduction

The field of evolutionary dynamics combines game theory and nonlinear dynamics to model population shifts due to competition in biological and social situations. One standard paradigm [3, 9] uses the replicator equation,

$$\dot{x}_i = x_i(f_i(\mathbf{x}) - \phi), \quad i = 1, \dots, n \quad (14.1)$$

where x_i is the frequency, or relative abundance, of strategy i ; the unit vector \mathbf{x} is the vector of frequencies; $f_i(\mathbf{x})$ is the fitness of strategy i ; and ϕ is the average fitness, defined by

$$\phi = \sum_i x_i f_i(\mathbf{x}). \quad (14.2)$$

The replicator equation can be derived [10] from an exponential model of population growth,

$$\dot{\xi}_i = \xi_i f_i, \quad i = 1, \dots, n \quad (14.3)$$

where ξ_i is the population of strategy i , assuming that f_i depends only on the frequencies: $f_i = f_i(\mathbf{x})$. The derivation consists of a simple change of variables: $x_i \equiv \xi_i/p$ where $p = \sum_i \xi_i$ is the total population.

The game-theoretic component of the replicator model lies in the choice of fitness functions. Define the payoff matrix $A = (a_{ij})$ where a_{ij} is the expected reward for a strategy i individual vs. a strategy j individual. We assume the population

E. Wesson (✉)
Center for Applied Mathematics, Cornell University, Ithaca, NY 14853, USA
e-mail: enw27@cornell.edu

R. Rand
Cornell University, Ithaca, NY 14853, USA

is well-mixed, so that any individual competes against each strategy at a rate proportional to that strategy's frequency in the population. Then the fitness f_i is the total expected payoff for strategy i vs. all strategies:

$$f_i(\mathbf{x}) = (A\mathbf{x})_i = \sum_j a_{ij}x_j. \quad (14.4)$$

In this work, we generalize the replicator model to systems in which the payoff coefficients are quasiperiodic functions of time. Previous work by Ruelas and Rand [7, 8] investigated the Rock-Paper-Scissors replicator dynamics problem with periodic forcing of the payoff coefficients. We also consider a forced Rock-Paper-Scissors system. The quasiperiodically forced replicator model may find applications in biological or social systems where competition is affected by cyclical processes on different scales, such as days/years or weeks/years.

14.2 The Model

14.2.1 Rock-Paper-Scissors Games with Quasiperiodic Forcing

Rock-Paper-Scissors (RPS) games are a class of three-strategy evolutionary games in which each strategy is neutral vs. itself, and has a positive expected payoff vs. one of the other strategies and a negative expected payoff vs. the remaining strategy. The payoff matrix is thus

$$A = \begin{pmatrix} 0 & -b_2 & a_1 \\ a_2 & 0 & -b_3 \\ -b_1 & a_3 & 0 \end{pmatrix}. \quad (14.5)$$

We perturb off of the canonical case, $a_1 = \dots = b_3 = 1$, by taking

$$A = \begin{pmatrix} 0 & -1 - F(t) & 1 + F(t) \\ 1 & 0 & -1 \\ -1 & 1 & 0 \end{pmatrix} \quad (14.6)$$

where the forcing function F is given by

$$F(t) = \epsilon((1 - \delta) \cos \omega_1 t + \delta \cos \omega_2 t). \quad (14.7)$$

For ease of notation, write $(x_1, x_2, x_3) = (x, y, z)$. The dynamics occur in the simplex

$$S \equiv \{(x, y, z) \in \mathbb{R} \mid x, y, z \in [0, 1]\} \quad (14.8)$$

but since x, y, z are the frequencies of the three strategies, and hence $x + y + z = 1$, we can eliminate z using $z = 1 - x - y$. Therefore, the region of interest is T , the projection of S into the $x - y$ plane:

$$T \equiv \{(x, y) \in \mathbb{R} \mid x, y, x + y \in [0, 1]\}. \quad (14.9)$$

See Fig. 14.1. Thus the replicator equation (14.1) becomes

$$\dot{x} = -x(x + 2y - 1)(1 + (x - 1)F(t)) \quad (14.10)$$

$$\dot{y} = y(2x + y - 1 - x(x + 2y - 1)F(t)) \quad (14.11)$$

Note that $\dot{x} = 0$ when $x = 0$, $\dot{y} = 0$ when $y = 0$, and

$$\dot{x} + \dot{y} = (x + y - 1)(xF(t)(x + 2y - 1) - x + y) \quad (14.12)$$

so that $\dot{x} + \dot{y} = 0$ when $x + y = 1$, which means that $x + y = 1$ is an invariant manifold. This shows that the boundary of T is invariant, so trajectories cannot escape the region of interest.

Fig. 14.1 A curve in S and its projection in T

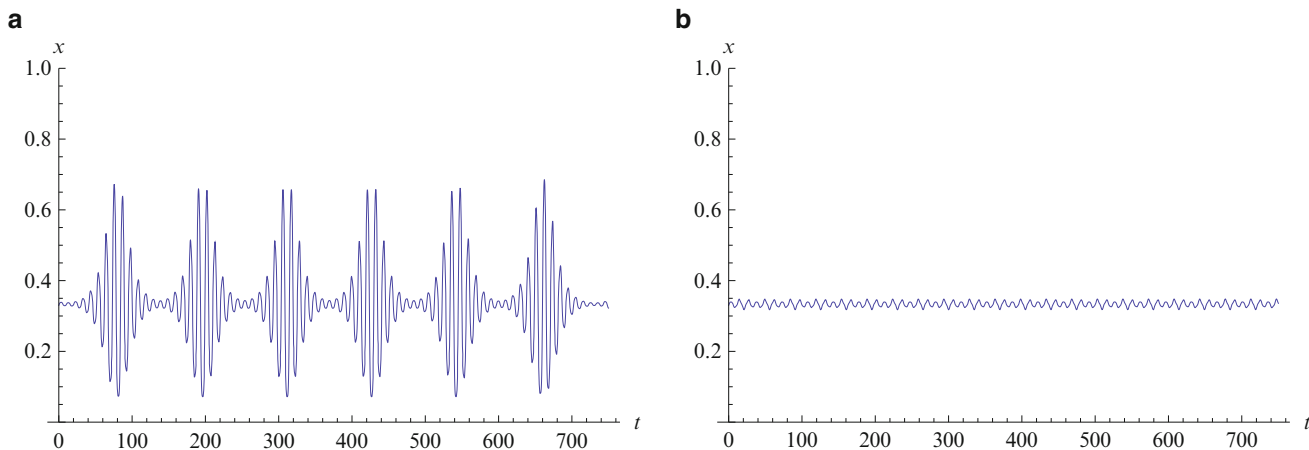
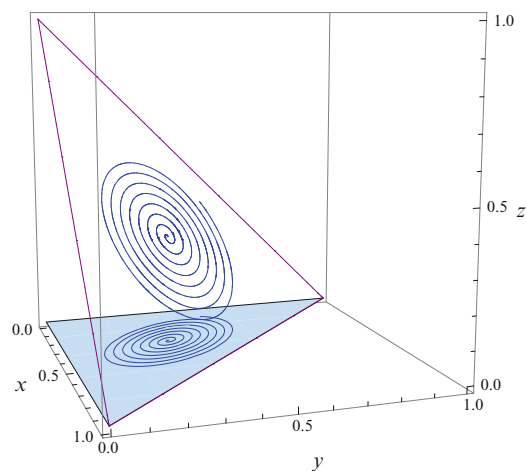


Fig. 14.2 Numerical solutions for $x(t)$ with identical initial conditions $x(0) = y(0) = 0.33$ and parameters $\epsilon = 0.9, \delta = 0.6$, but with different ω_1, ω_2 . **(a)** $\omega_1 = \omega_2 = 1.2$. **(b)** $\omega_1 = \omega_2 = 0.9$

It is known [4] that in the unperturbed case ($\epsilon = 0$) there is an equilibrium point at $(x, y) = (\frac{1}{3}, \frac{1}{3})$, and the interior of T is filled with periodic orbits. We see from Eqs. (14.10)–(14.11) that this interior equilibrium point persists when $\epsilon \neq 0$. Numerical integration suggests that the Lyapunov stability of motions around the equilibrium point depends sensitively on the values of ω_1 and ω_2 . See Fig. 14.2. We investigate the stability of the interior equilibrium using Floquet theory and harmonic balance, as well as by numerical methods.

14.2.2 Linearization

To study the linear stability of the equilibrium point, we set $x = u + \frac{1}{3}, y = v + \frac{1}{3}$, substitute these into (14.10)–(14.11) and linearize, to obtain

$$\dot{u} = -\frac{1}{9}(u + 2v)(3 + 2F(t)) \tag{14.13}$$

$$\dot{v} = \frac{1}{9}(F(t)(u + 2v) + 3(2u + v)). \tag{14.14}$$

The linearized system (14.13)–(14.14) can also be written [6] as a single second-order equation on u , by differentiating (14.13) and substituting in expressions for \dot{v} from (14.14) and v from (14.13). This gives us

$$g(t)\ddot{u} - \dot{g}(t)\dot{u} - \frac{1}{9}g^2(t)u = 0 \quad (14.15)$$

where

$$g(t) = -3 - 2F(t) = -3 - 2\epsilon((1 - \delta)\cos\omega_1 t + \delta\cos\omega_2 t). \quad (14.16)$$

Now that we have a linear system with coefficients that are functions of time, we use Floquet theory to determine the stability of the origin.

14.3 Floquet Theory

Floquet theory is concerned with systems of differential equations of the form

$$\frac{dx}{dt} = M(t)x, \quad M(t + T) = M(t). \quad (14.17)$$

We have the system (14.13)–(14.14), which can be written as

$$\begin{bmatrix} \dot{u} \\ \dot{v} \end{bmatrix} = \frac{1}{9} \begin{bmatrix} g(t) & 2g(t) \\ \frac{1}{2}(9 - g(t)) & -g(t) \end{bmatrix} \begin{bmatrix} u \\ v \end{bmatrix} \equiv B(t) \begin{bmatrix} u \\ v \end{bmatrix} \quad (14.18)$$

where $g(t)$ is as in (14.16).

In general, $B(t)$ is not periodic, since ω_1 and ω_2 are rationally independent. However, the set of points for which ω_1 and ω_2 are rationally dependent is dense in the $\omega_1 - \omega_2$ plane, and solutions of (14.18) must vary continuously with ω_1 and ω_2 , so it is reasonable to consider only the case that $F(t)$, and hence $g(t)$ and $B(t)$, are in fact periodic.

Assume that $\omega_2 = \frac{a}{b}\omega_1$ in lowest terms, where a and b are relatively prime integers. Then we can make the change of variables $\tau = \omega_1 t$, so $\omega_2 t = \frac{a}{b}\tau$. Since a and b are relatively prime, we see that F , and hence g and B , have period $T = 2\pi b$ in τ . Thus (14.18) becomes

$$\begin{bmatrix} u' \\ v' \end{bmatrix} = \frac{1}{\omega_1} B(\tau) \begin{bmatrix} u \\ v \end{bmatrix}, \quad B(\tau + 2\pi b) = B(\tau) \quad (14.19)$$

where u' indicates $du/d\tau$. This has the same form as (14.17), so we can apply the results of Floquet theory.

Suppose that there is a fundamental solution matrix of (14.19),

$$X(\tau) = \begin{bmatrix} u_1(\tau) & u_2(\tau) \\ v_1(\tau) & v_2(\tau) \end{bmatrix} \quad (14.20)$$

where

$$\begin{bmatrix} u_1(0) \\ v_1(0) \end{bmatrix} = \begin{bmatrix} 1 \\ 0 \end{bmatrix}, \quad \begin{bmatrix} u_2(0) \\ v_2(0) \end{bmatrix} = \begin{bmatrix} 0 \\ 1 \end{bmatrix}. \quad (14.21)$$

Then the Floquet matrix is $C = X(T) = X(2\pi b)$, and stability is determined by the eigenvalues of C :

$$\lambda^2 - (\text{tr}C)\lambda + \det C = 0. \quad (14.22)$$

We can show [5] that $\det C = 1$, as follows. Define the Wronskian

$$W(\tau) = \det X(\tau) = u_1(\tau)v_2(\tau) - u_2(\tau)v_1(\tau). \quad (14.23)$$

Notice that $W(0) = \det X(0) = 1$. Then taking the time derivative of W and using (14.19) gives

$$\begin{aligned} \frac{dW}{d\tau} &= u'_1(\tau)v_2(\tau) + u_1(\tau)v'_2(\tau) - u'_2(\tau)v_1(\tau) - u_2(\tau)v'_1(\tau) \\ &= \frac{1}{9\omega_1} \left(g(\tau)(u_1 + 2v_1)v_2 + \frac{1}{2}u_1(9u_2 - (u_2 + 2v_2)g(\tau)) \right. \\ &\quad \left. - g(\tau)(u_2 + 2v_2)v_1 - \frac{1}{2}u_2(9u_1 - (u_1 + 2v_1)g(\tau)) \right) = 0. \end{aligned} \quad (14.24)$$

This shows that $W(\tau) = 1$ for all τ , and in particular $W(T) = \det C = 1$. Therefore,

$$\lambda = \frac{\text{tr}C \pm \sqrt{\text{tr}C^2 - 4}}{2} \quad (14.25)$$

which means [5] that the transition between stable and unstable solutions occurs when $|\text{tr}C| = 2$, and this corresponds to periodic solutions of period $T = 2\pi b$ or $2T = 4\pi b$.

Given the period of the solutions on the transition curves in the $\omega_1 - \omega_2$ plane, we use harmonic balance to approximate those transition curves.

14.4 Harmonic Balance

We seek solutions to (14.15) of period $4\pi b$ in τ :

$$u = \sum_{k=0}^{\infty} \alpha_k \cos\left(\frac{k\tau}{2b}\right) + \beta_k \sin\left(\frac{k\tau}{2b}\right). \quad (14.26)$$

Since $\omega_2 = \frac{a}{b}\omega_1$ where a and b are relatively prime, any integer k can be written as $na + mb$ for some integers n and m [2, 11]. That is, there is a one-to-one correspondence between integers k and ordered pairs (m, n) . We can therefore write the solution as

$$u = \sum_{m=0}^{\infty} \sum_{n=-\infty}^{\infty} \alpha_{mn} \cos\left(\frac{ma + nb}{2b}\tau\right) + \beta_{mn} \sin\left(\frac{ma + nb}{2b}\tau\right) \quad (14.27)$$

$$= \sum_{m=0}^{\infty} \sum_{n=-\infty}^{\infty} \alpha_{mn} \cos\left(\frac{m\omega_2 + n\omega_1}{2}t\right) + \beta_{mn} \sin\left(\frac{m\omega_2 + n\omega_1}{2}t\right). \quad (14.28)$$

We substitute a truncated version of (14.28) into (14.15), expand the trigonometric functions and collect like terms. This results in cosine terms whose coefficients are functions of the α_{mn} , and sine terms whose coefficients are functions of the β_{mn} . Let the coefficient matrices of these two sets of terms be Q and R , respectively. In order for a nontrivial solution to exist, the determinants of both coefficient matrices must vanish [5]. We solve the equations $\det Q = 0$ and $\det R = 0$ for relations between ω_1 and ω_2 . This gives the approximate transition curves seen in Fig. 14.3.

It has been shown [6, 7] that in a periodically forced RPS system (i.e. $\delta = 0$ in our model) there are tongues of instability emerging from $\omega_1 = 2/n\sqrt{3}$ in the $\omega_1 - \epsilon$ plane. Our harmonic balance analysis is consistent with this: we observe bands of instability around $\omega_1 = 2/\sqrt{3}$ and $\omega_2 = 2/\sqrt{3}$, which get broader as ϵ increases. We also see narrower regions of instability along the lines $n\omega_1 + m\omega_2 = 2/\sqrt{3}$, for each n, m used in the truncated solution (14.28).

Thus the boundary of the region of instability exhibits self-similarity when we consider $\omega_1, \omega_2 \in [0, 2^{1-k}]$ for $k = 0, 1, \dots$

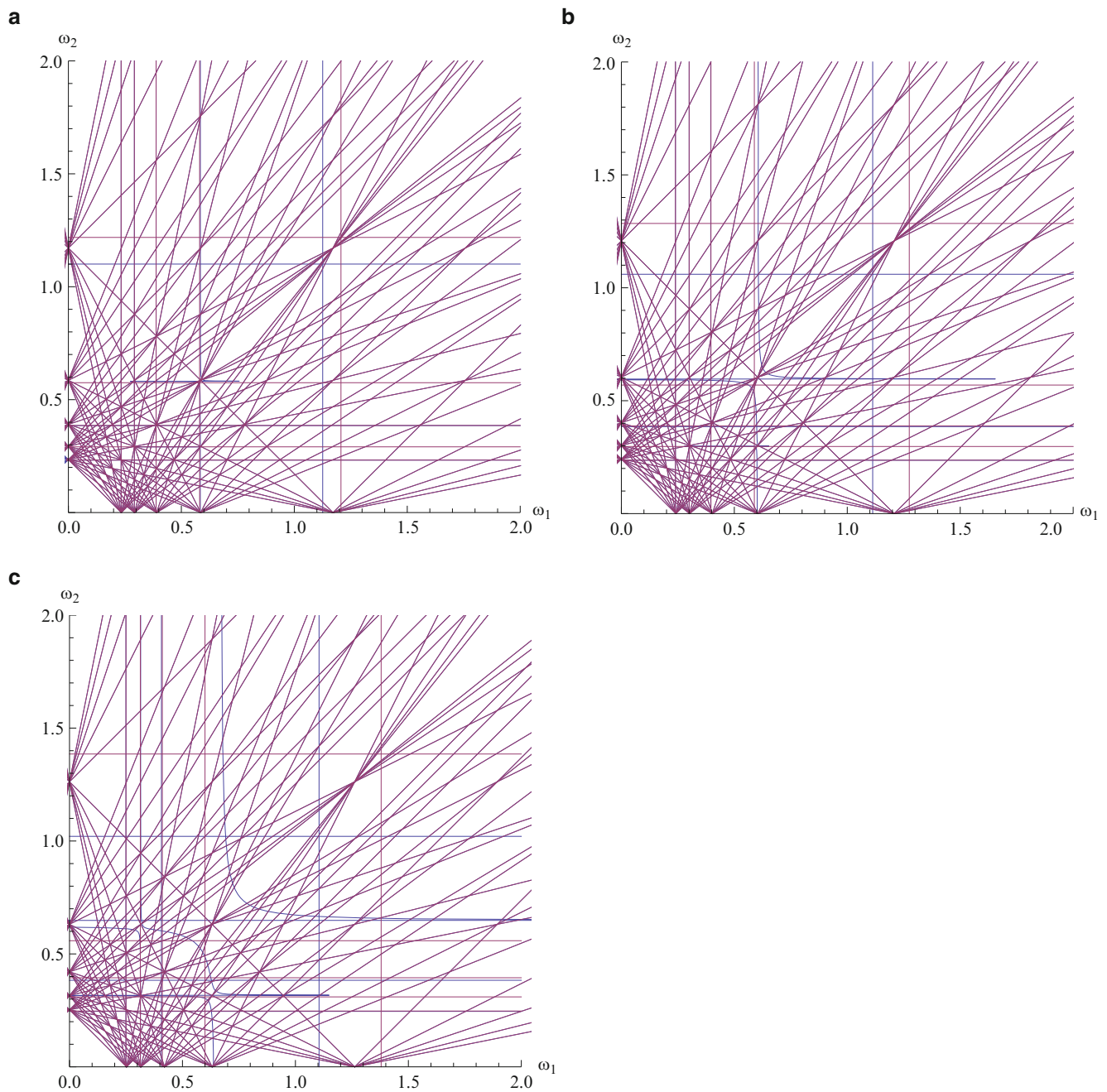


Fig. 14.3 Transition curves predicted by harmonic balance with $-5 \leq m \leq 5$, $0 \leq n \leq 5$ for various values of ϵ . (a) $\epsilon = 0.5$, $\delta = 0.6$. (b) $\epsilon = 0.9$, $\delta = 0.6$. (c) $\epsilon = 1.3$, $\delta = 0.6$

14.5 Numerical Integration

In order to check the results of the harmonic balance method, we generate an approximate stability diagram by numerical integration of the linearized system (14.15).

For randomly chosen parameters $(\omega_1, \omega_2) \in [0, 2]$, we choose random initial conditions $(u(0), \dot{u}(0))$ on the unit circle—since the system is linear, the amplitude of the initial condition needs only to be consistent between trials. We then integrate the system for 1,000 time steps using `ode45` in Matlab. This is an explicit Runge-Kutta (4,5) method that is recommended in the Matlab documentation for most non-stiff problems. We considered a motion to be unstable if $\max |u(t)| > 10$. The set

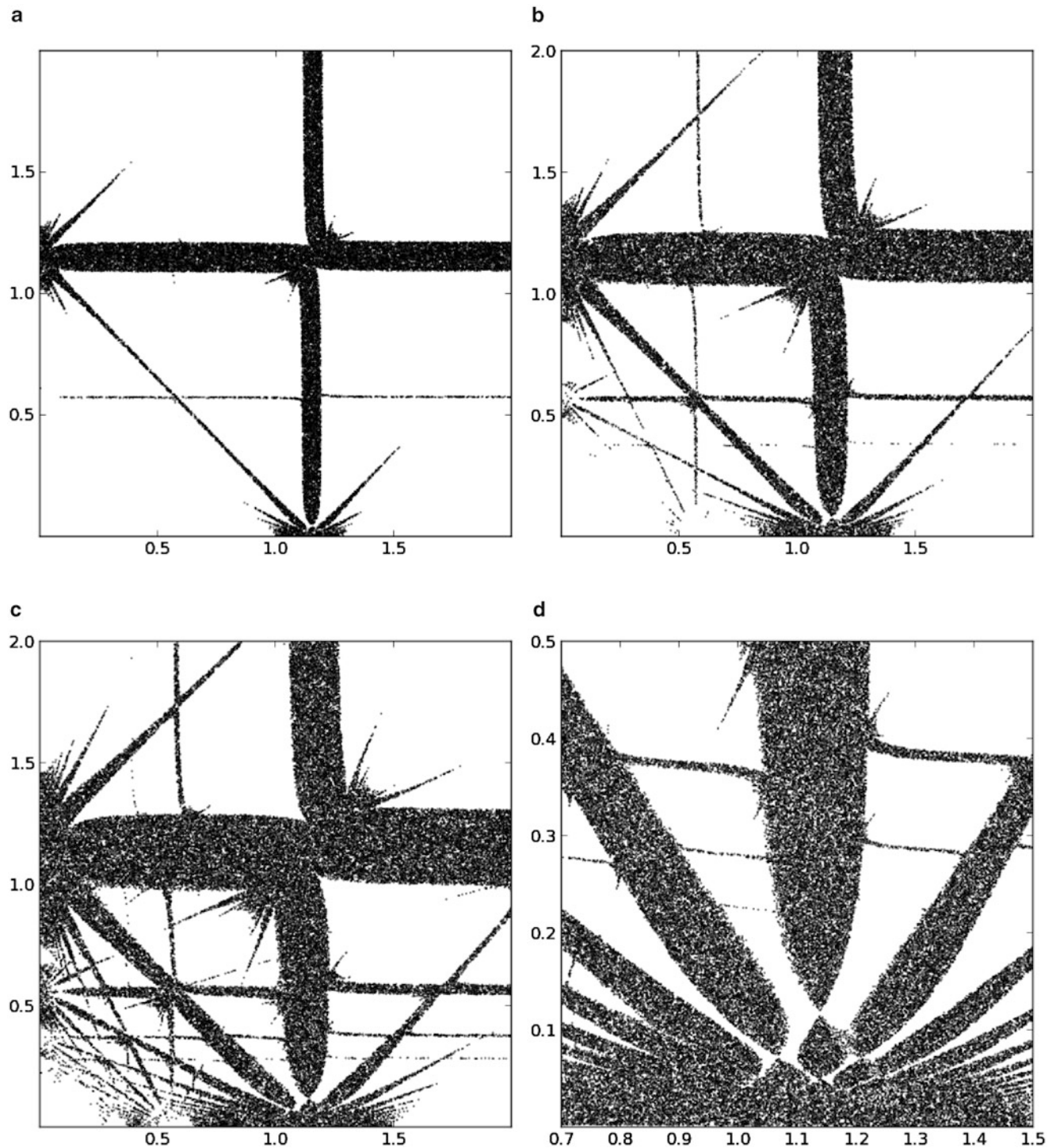


Fig. 14.4 Plots of unstable points in the (ω_1, ω_2) plane for various values of ϵ . (a) $\epsilon = 0.5, \delta = 0.6$. (b) $\epsilon = 0.9, \delta = 0.6$. (c) $\epsilon = 1.3, \delta = 0.6$. (d) Detail view: $\epsilon = 1.3, \delta = 0.6$

of points (ω_1, ω_2) corresponding to unstable motions were plotted using `matplotlib.pyplot` in Python. See Fig. 14.4. Each plot in Fig. 14.4 contains approximately 5×10^4 points.

We note that the unstable regions given by numerical integration appear to be consistent with the transition curves predicted by harmonic balance (Fig. 14.3). The regions of instability around $\omega_1 = 2/\sqrt{3}$ and $\omega_2 = 2/\sqrt{3}$ are visible for all tested values of ϵ and δ , and as ϵ increases, more tongues of the form $n\omega_1 + m\omega_2 = 2/\sqrt{3}$ become visible.

14.6 Lyapunov Exponents

A second, and more informative, numerical approach for determining stability is the computation of approximate Lyapunov exponents. This is a measure of a solution's rate of divergence from the equilibrium point [1], and is defined as

$$\lambda = \limsup_{t \rightarrow \infty} \frac{1}{t} \ln |u(t)|. \quad (14.29)$$

If the limit is finite, then $u(t) \sim e^{\lambda t}$ or smaller as $t \rightarrow \infty$. A positive Lyapunov exponent indicates that the solution is unstable.

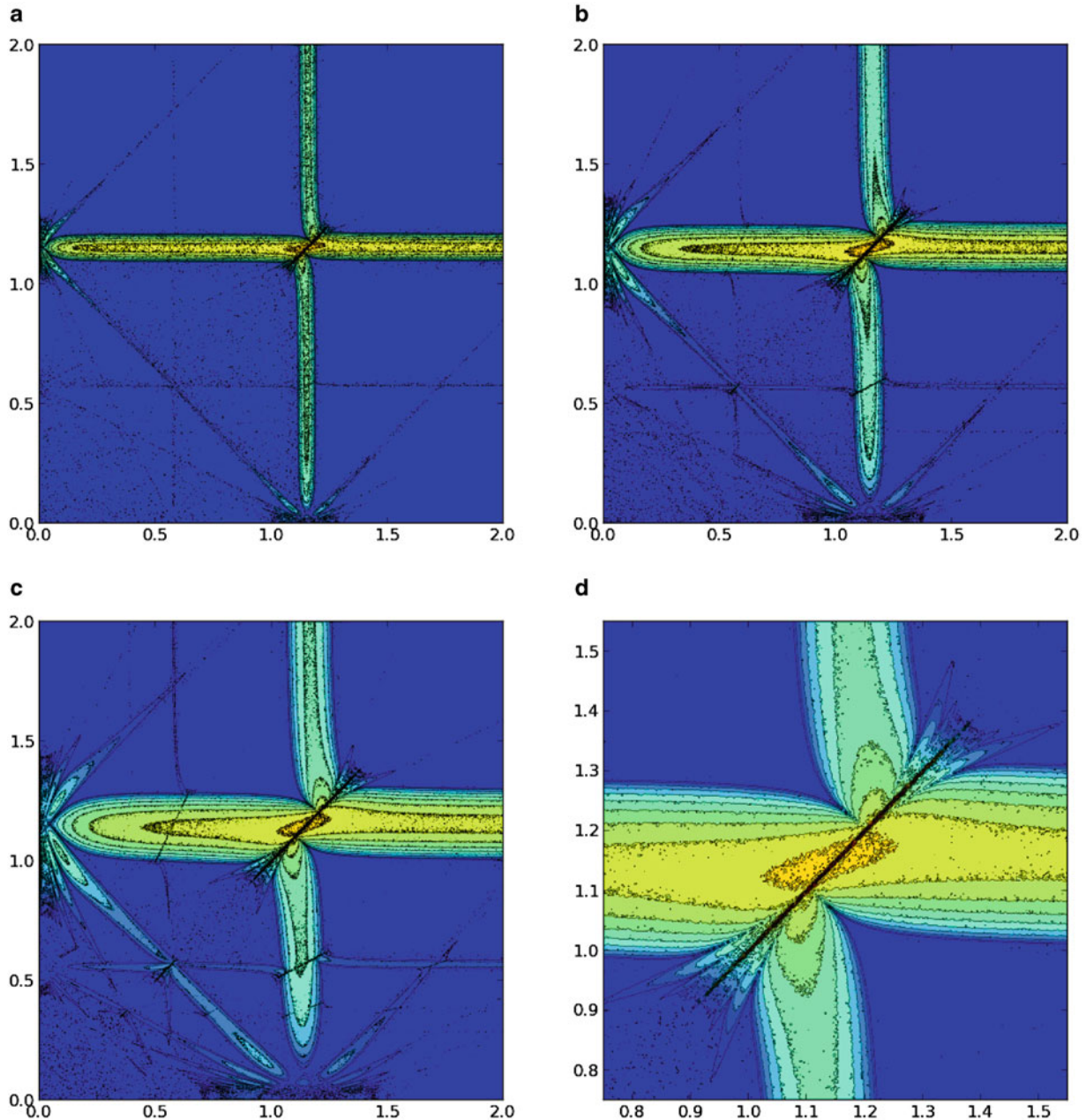


Fig. 14.5 Contour plot of Lyapunov exponents in the (ω_1, ω_2) plane for various values of ϵ . (a) $\epsilon = 0.5, \delta = 0.6$. Contours between $\lambda = 0$ and $\lambda = 0.04$. (b) $\epsilon = 0.9, \delta = 0.6$. Contours between $\lambda = 0$ and $\lambda = 0.08$. (c) $\epsilon = 1.3, \delta = 0.6$. Contours between $\lambda = 0$ and $\lambda = 0.12$. (d) Detail view: $\epsilon = 1.3, \delta = 0.6$. Contours as in (c)

We do not find any negative Lyapunov exponents, but note [5] that the system (14.15) can be converted to a Hill's equation

$$\ddot{z} - z \left(\frac{4g(t)^3 + 27\dot{g}(t)^2 - 18g(t)\ddot{g}(t)}{36g(t)^2} \right) = 0 \quad (14.30)$$

by making the change of variables $u = \sqrt{g(t)}z$. Since $\sqrt{g(t)}$ is bounded, u is bounded if and only if z is bounded. And since there is no dissipation in (14.30), stable solutions correspond to $\lambda = 0$.

We approximate the Lyapunov exponents numerically by integrating as above, and taking

$$\lambda \approx \sup_{900 < t < 1000} \frac{1}{t} \ln |u(t)|. \quad (14.31)$$

See Fig. 14.5. The shape of the unstable region is the same as in Fig. 14.4, but this method allows us to see a sharp increase in unstable solutions' rate of growth along the line $\omega_1 = \omega_2$.

14.7 Conclusion

The replicator equation with quasiperiodic perturbation may be used to model biological or social systems where competition is affected by cyclical processes on different scales. We have investigated the linear stability of the interior equilibrium point for RPS systems with quasiperiodic perturbation, using Floquet theory and harmonic balance, as well as numerical integration and numerical computation of Lyapunov exponents. We find that stability depends sensitively on the frequencies ω_1 and ω_2 , and that the region of instability in the $\omega_1 - \omega_2$ plane exhibits self-similarity.

References

1. Guckenheimer J, Holmes P (1983) Nonlinear oscillations, dynamical systems, and bifurcations of vector fields. Springer, New York
2. Herstein I (1975) Topics in algebra, 2nd edn. Wiley, New York
3. Hofbauer J, Sigmund K (1998) Evolutionary games and population dynamics. Cambridge University Press, Cambridge
4. Nowak M (2006) Evolutionary dynamics. Belknap Press of Harvard University Press, Cambridge, MA
5. Rand R (2012) Lecture notes on nonlinear vibrations. Published online by The Internet-First University Press. <http://ecommons.library.cornell.edu/handle/1813/28989>
6. Rand R, Yazhbin M, Rand D (2011) Evolutionary dynamics of a system with periodic coefficients. Commun Nonlinear Sci Numer Simul 16:3887–3895
7. Ruelas R, Rand D, Rand R (2012) Nonlinear parametric excitation of an evolutionary dynamical system. J. Mech Eng Sci Proc Inst Mech Eng C 226:1912–1920
8. Ruelas R, Rand D, Rand R (2013) Parametric excitation and evolutionary dynamics. J Appl Mech 80:051013
9. Sigmund K (2011) Introduction to evolutionary game theory, Chap. 1. In: Sigmund K (ed) Evolutionary game dynamics. Proceedings of symposia in applied mathematics, vol 69, pp 1–26. American Mathematical Society, Providence
10. Taylor P, Jonker L (1978) Evolutionarily stable strategies and game dynamics. Math Biosci 40(1–2):145–156
11. Zounes R, Rand R (1998) Transition curves for the quasi-periodic mathieu equation. Siam J Appl Math 40(4): 1094–1115